RECOMMENDATION ITU-R P.680-3

PROPAGATION DATA REQUIRED FOR THE DESIGN OF EARTH-SPACE MARITIME MOBILE TELECOMMUNICATION SYSTEMS

(Question ITU-R 207/3)

(1990-1992-1997-1999)

The ITU Radiocommunication Assembly,

considering

a) that for the proper planning of Earth-space maritime mobile systems it is necessary to have appropriate propagation data and prediction methods;

b) that the methods of Recommendation ITU-R P.618 are recommended for the planning of Earth-space telecommunication systems;

c) that further development of prediction methods for specific application to maritime mobile-satellite systems is required to give adequate accuracy for all operational conditions;

d) that, however, methods are available which yield sufficient accuracy for many applications,

recommends

1 that the current methods set out in Annex 1 be adopted for use in the planning of Earth-space maritime mobile telecommunication systems, in addition to the methods recommended in Recommendation ITU-R P.618.

ANNEX 1

1 Introduction

Telecommunications over Earth-space links for maritime mobile-satellite systems lead to propagation problems that are substantially different from those arising in the fixed-satellite service. For instance, the effects of reflections and scattering by the sea surface can be quite severe, in particular where antennas with wide beamwidths are used. Furthermore, maritime mobile-satellite systems may operate on a world-wide basis, including paths with low elevation angles.

This Annex deals with data and models specifically needed to characterize the sea-space path impairments which include:

– tropospheric effects, including rain attenuation, gaseous absorption, refraction, scintillation and anomalous propagation occurring at low elevation angles;

– ionospheric effects such as scintillation and Faraday rotation;

– surface reflection effects (multipath due to secondary paths arising from the reflection of radio waves from the sea surface);

– local environment effects (ship motion and sea conditions);

– interference effects due to differential fading between a desired signal and an interference signal, both affected by multipath fading.

2 Tropospheric effects

2.1 Attenuation

Signal losses in the troposphere are caused by atmospheric gases, rain, fog and clouds. Except at low elevation angles, tropospheric attenuation is negligible at frequencies below about 1 GHz, and is generally small at frequencies up to about 10 GHz. Above 10 GHz, the attenuation can be large for significant percentages of the time on many paths.

Prediction methods are available for estimating gaseous absorption (see Recommendation ITU-R P.676) and rain attenuation (see Recommendation ITU-R P.618). Fog and cloud attenuation is usually negligible for frequencies up to 10 GHz.

2.2 Scintillation

Irregular variations in received signal level and in angle of arrival are caused by both tropospheric turbulence and atmospheric multipath. The magnitudes of these effects increase with increasing frequency and decreasing path elevation angle, except that angle of arrival fluctuations caused by turbulence are independent of frequency. Antenna beamwidth also affects the magnitude of these scintillations. These effects are observed to be at a maximum in the summer season. A prediction method is given in Recommendation ITU-R P.618.

3 Ionospheric effects

Ionospheric effects (see Recommendation ITU-R P.531) may be important, particularly at frequencies below 1 GHz. For convenience these have been quantified for frequencies of 0.1, 0.25, 0.5, 1, 3 and 10 GHz in Table 1 for a high value of total electron content (TEC).

3.1 Ionospheric scintillation

Inhomogeneities of electron density in the ionosphere cause refractive focusing or defocusing of radio waves and lead to amplitude fluctuations termed scintillations. Ionospheric scintillation is maximum near the geomagnetic equator and smallest in the mid-latitude regions. The auroral zones are also regions of large scintillation. Strong scintillation is Rayleigh distributed in amplitude; weaker scintillation is nearly log-normal. These fluctuations decrease with increasing frequency and depend upon path geometry, location, season, solar activity and local time. Table 2 tabulates fade depth data for VHF and UHF in mid-latitudes, based on data in Recommendation ITU-R P.531.

Accompanying the amplitude fluctuation is also a phase fluctuation. The spectral density of the phase fluctuation is proportional to $1/f^3$, where f is the Fourier frequency of the fluctuation. This spectral characteristic is similar to that arising from flicker of frequency in oscillators and can cause significant degradation to the performance of receiver hardware.

3.2 Faraday rotation

A linearly polarized wave propagating through the ionosphere undergoes a progressive rotation of the plane of polarization. Effects are summarized in Table 1.

The axial ratio of an incident elliptically polarized wave may be increased or decreased upon reflection (particularly at small angles) since Faraday rotation varies the orientation of the principal polarization axis of the incident wave. This results from the difference in reflection coefficient to be expected between vertical and horizontal components in most multipath situations.

The effects of Faraday rotation on wideband signals can be of significance to system performance. The differential rotation effects cannot be fully corrected at VHF by reorientation of the antenna axis of a linearly polarized antenna. On circularly polarized antennas, the effect is to introduce differential phase shifts of signal components across the band. Thus, signal components separated in frequency may be expected to be subject to frequency and phase selective distortion.

TABLE 1

Estimated* ionospheric effects for elevation angles of about 30° one-way traversal**

(derived from Recommendation ITU-R P.531)

Effect	Frequency dependence	0.1 GHz	0.25 GHz	0.5 GHz	1 GHz	3 GHz	10 GHz
Faraday rotation	$1/f^2$	30 rotations	4.8 rotations	1.2 rotations	108°	12°	1.1°
Propagation delay	$1/f^2$	25 μs	4 μs	1 μs	0.25 μs	0.028 μs	0.0025 μs
Refraction	$1/f^2$	< 1°	< 0.16°	< 2.4′	< 0.6′	< 4.2″	< 0.36″
Variation in the direction of arrival (r.m.s.)	$1/f^2$	20′	3.2′	48″	12″	1.32″	0.12″
Absorption (auroral and/or polar cap)	$\approx 1/f^2$	5 dB	0.8 dB	0.2 dB	0.05 dB	6×10^{-3} dB	5×10^{-4} dB
Absorption (mid-latitude)	$1/f^2$	< 1 dB	< 0.16 dB	< 0.04 dB	< 0.01 dB	< 0.001 dB	$< 10^{-4}$ dB
Dispersion	$1/f^3$	0.4 ps/Hz	0.026 ps/Hz	0.0032 ps/Hz	0.0004 ps/Hz	1.5×10^{-5} ps/Hz	4×10^{-7} ps/Hz
Scintillation (1)	See Rec. ITU-R.P.531	See Rec. ITU-R P.531	See Rec. ITU-R P.531	See Rec. ITU-R P.531	>20 dB peak-to-peak	≈ 10 dB peak-to-peak	≈ 4 dB peak-to-peak

* This estimate is based on a TEC of 10^{18} electrons/m^2, which is a high value of TEC encountered at low latitudes in day-time with high solar activity.

** Ionospheric effects above 10 GHz are negligible.

(1) Values observed near the geomagnetic equator during the early night-time hours (local time) at equinox under conditions of high sunspot number.

TABLE 2

Distribution of mid-latitude fade depths due to ionospheric scintillation (dB)

Percentage of time (%)	Frequency (GHz)			
	0.1	0.2	0.5	1
1.0	5.9	1.5	0.2	0.1
0.5	9.3	2.3	0.4	0.1
0.2	16.6	4.2	0.7	0.2
0.1	25.0	6.2	1.0	0.3

4 Fading due to sea reflection

4.1 Fading depth

The following simple method provides approximate estimates of multipath power or fading depth suitable for many engineering applications.

Applicable conditions:

Frequency range: 0.8-8 GHz

Elevation angle: $5° \le \theta_i \le 20°$

where $G(\theta)$ is the antenna radiation pattern of the main lobe given by:

$$G(\theta) = -4 \times 10^{-4} \, (10^{G_m/10} - 1) \, \theta^2 \qquad \text{dBi} \tag{1}$$

where:

G_m: value of the maximum antenna gain (dBi)

θ: angle measured from boresight (degrees)

Polarization: circular

Sea condition: wave height of 1-3 m (incoherent component fully developed).

Step 1: Find the relative antenna gain G in the direction of the point of specular reflection. The relative antenna gain is approximated by equation (1) where $\theta = 2\,\theta_i$ (degrees).

Step 2: Calculate the Fresnel reflection coefficient of the sea for circular polarization, R_C:

$$R_C = \frac{R_H + R_V}{2} \qquad \text{(circular polarization)} \tag{2a}$$

where:

$$R_H = \frac{\sin\theta_i - \sqrt{\eta - \cos^2\theta_i}}{\sin\theta_i + \sqrt{\eta - \cos^2\theta_i}} \qquad \text{(horizontal polarization)} \tag{2b}$$

$$R_V = \frac{\sin\theta_i - \sqrt{(\eta - \cos^2\theta_i)/\eta^2}}{\sin\theta_i + \sqrt{(\eta - \cos^2\theta_i)/\eta^2}} \qquad \text{(vertical polarization)} \tag{2c}$$

and $\eta = \varepsilon_r(f) - j\,60\,\lambda\,\sigma(f)$

where:

$\varepsilon_r(f)$: relative permittivity of the surface at frequency f (from Recommendation ITU-R P.527)

$\sigma(f)$: conductivity (S/m) of the surface at frequency f (from Recommendation ITU-R P.527)

λ: free space wavelength (m).

A set of curves is given in Fig. 1 for the magnitude of the Fresnel reflection coefficient of sea for circular polarization for five frequencies between 0.8 GHz and 8 GHz. The curves are obtained from equation (2) with the electrical parameters corresponding to average salinity sea water.

Step 3: Find the normalized diffuse coefficient (ratio of diffuse component of reflection-to-reflection coefficient for calm sea condition), η_I (dB), from Fig. 2.

FIGURE 1

Magnitude of Fresnel reflection coefficient, R_C, of sea of average salinity for circular polarization

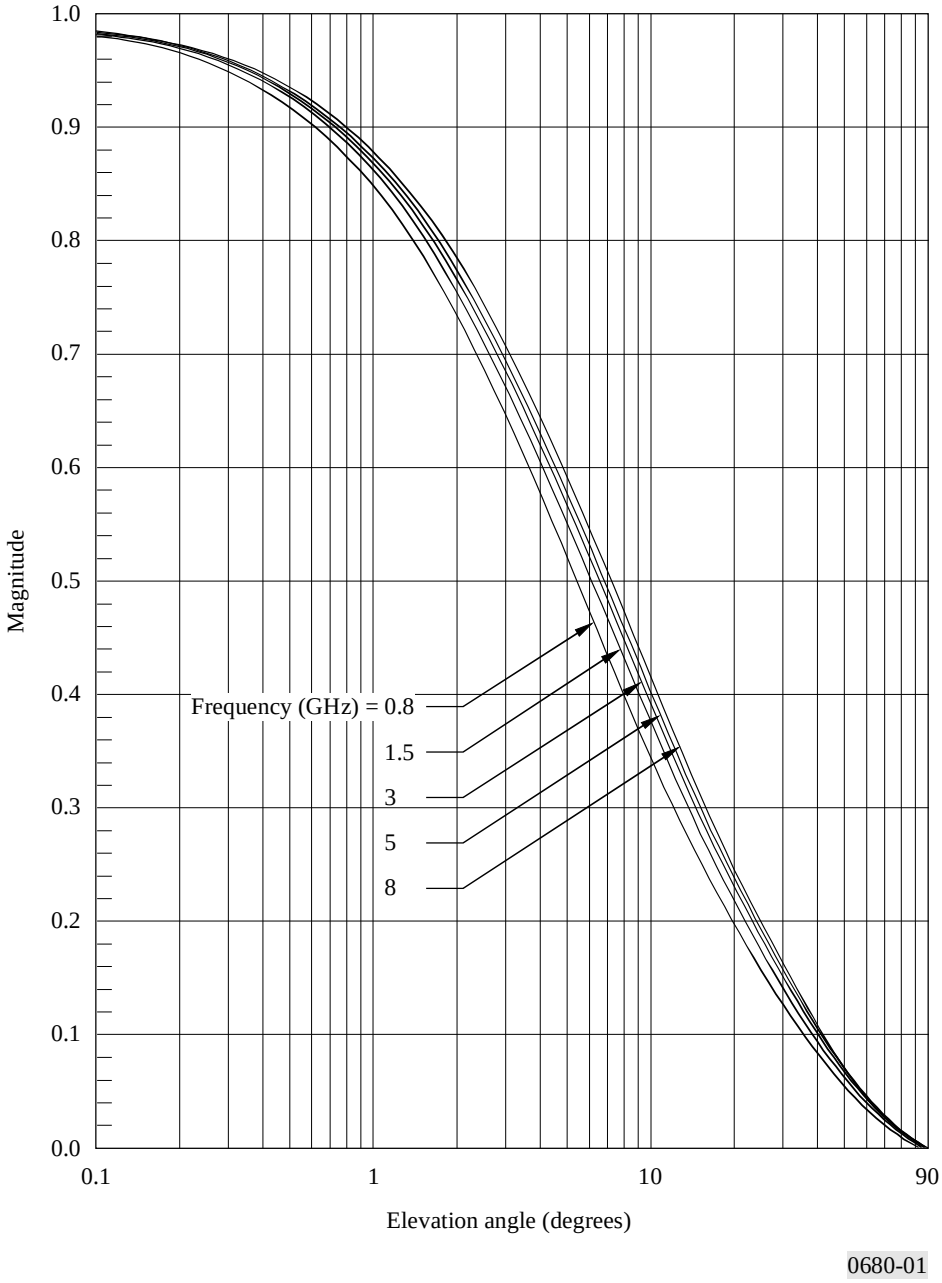

FIGURE 2

Average normalized diffuse coefficients in the range 0.8 to 8 GHz

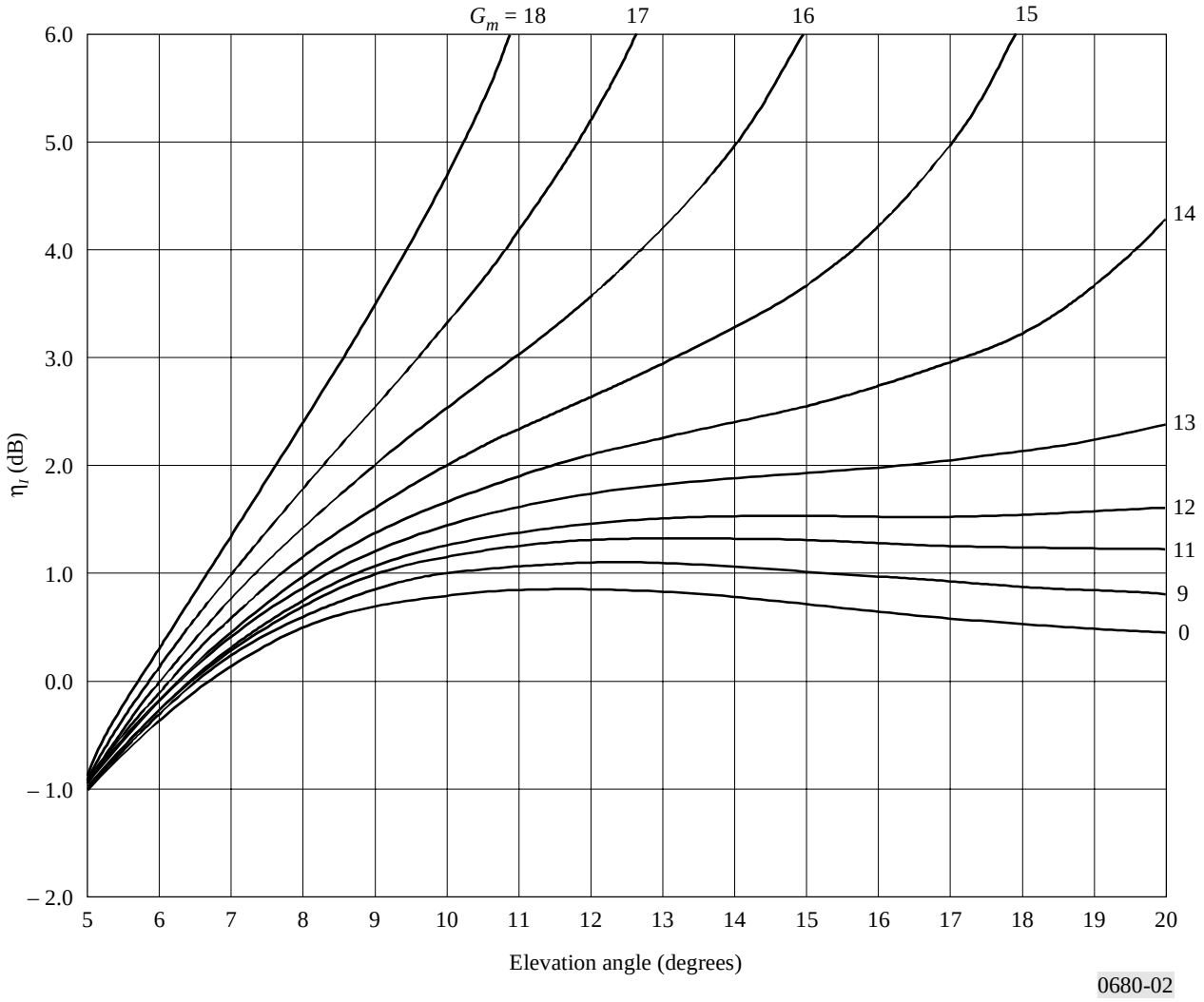

Step 4: The mean incoherent power of sea reflected waves relative to the direct wave, P_r, is given by:

$$P_r = G + R + \eta_I \quad \text{dB} \tag{3}$$

where:

$$R = 20 \log |R_C| \quad \text{dB} \tag{3a}$$

with R_C from equation (2).

Step 5: Assuming the Nakagami-Rice distribution, fading depth is estimated from:

$$A + 10 \log \left(1 + 10^{P_r / 10} \right) \tag{4}$$

where A is the amplitude (dB) read from the ordinate of Fig. 3.

FIGURE 3

Nakagami-Rice distribution for a constant total power with the parameter α

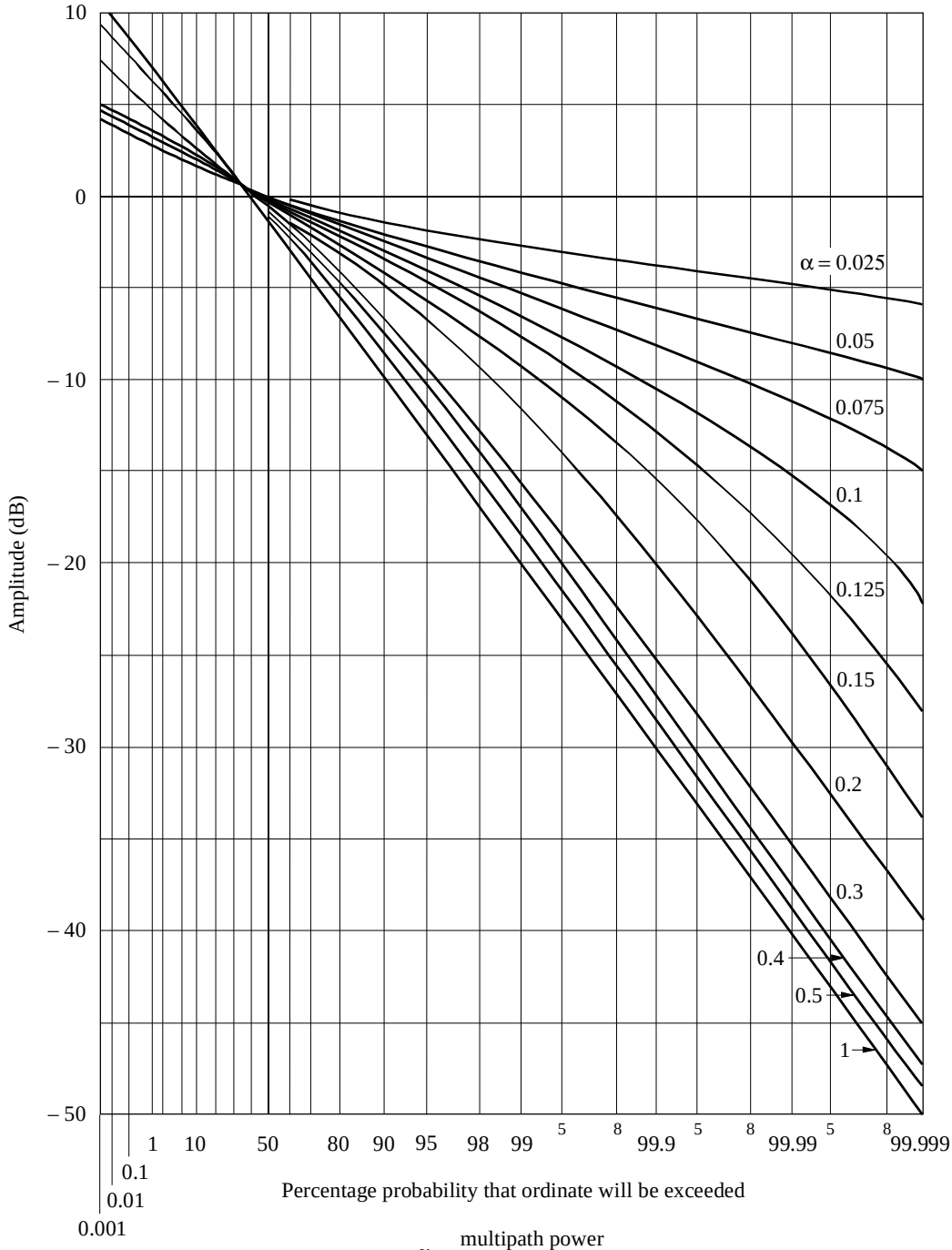

$$\alpha = \frac{\text{multipath power}}{\text{total power}}$$

For this case, $\alpha = \dfrac{10^{P_r/10}}{1 + 10^{P_r/10}}$

0680-03

4.2 Frequency spectrum and fade duration statistics

In general, spectral bandwidth increases with increasing wave height, elevation angle, ship velocity, and the relative motion of the shipborne antenna (rolling/pitching). The dependence of the spectral shape on antenna polarization is small, and the dependence on antenna gain is weak for gains less than about 10 dB.

The –10 dB spectral bandwidth, f_{-10}, is defined as the bandwidth over which the power density decays to –10 dB relative to the peak power density. Figure 4 shows the probable range of the -10 dB spectral bandwidth of 1.5 GHz multipath fading obtained by a theoretical fading model as a function of the elevation angle under conditions typical of maritime satellite communications (significant wave height of 1-5 m, ship speed of 0-20 knots and rolling of 0-30°).

FIGURE 4

–10 dB spectral bandwidth of 1.5 GHz multipath fading due to sea reflection as a function of the elevation angle

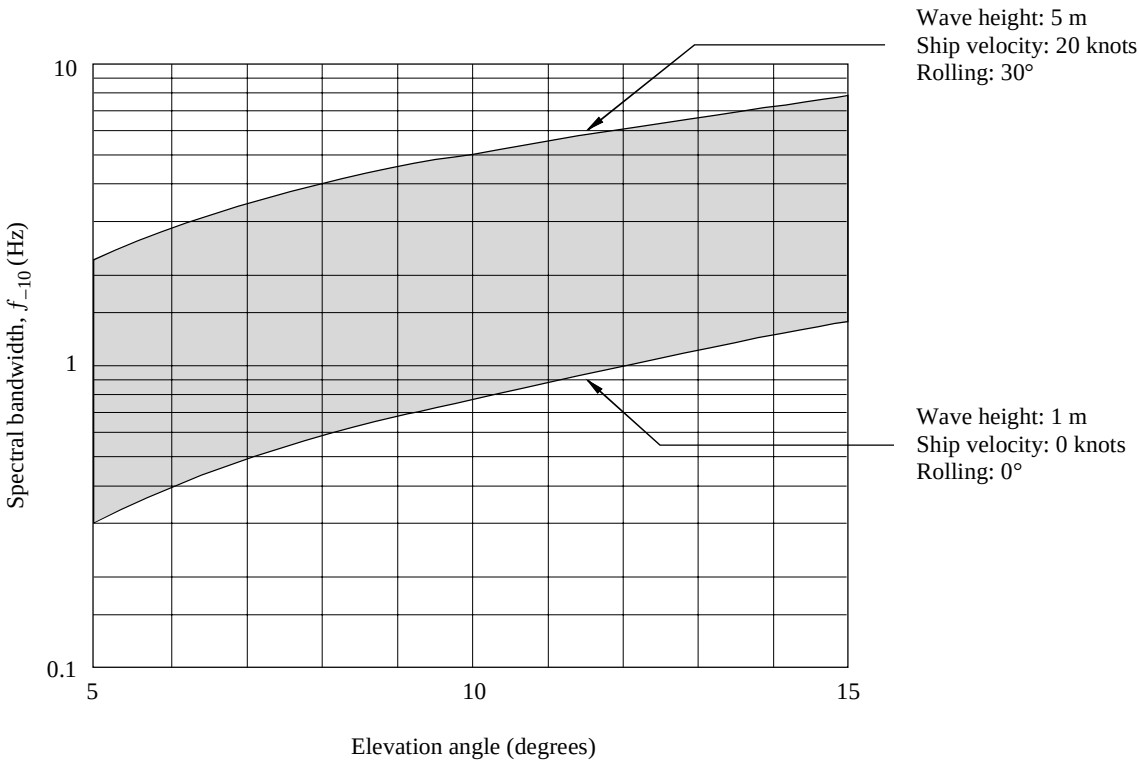

Average values of fade duration, $<T_D>$, and fade occurrence interval, $<T_I>$ defined in Fig. 5 can be obtained by the following procedure by using the –10 dB spectral bandwidth, f_{-10}:

$$< T_I (p) > = < T_I (50\%) > \exp \left[m(p)^2 / 2 \right]$$

$$< T_D (p) > = < T_I (p) > (1 - p / 100)$$

where:

$$< T_I (50\%) > = \sqrt{3} / f_{-10}$$

$$m = 2.33 - 0.847\, a - 0.144\, a^2 - 0.0657\, a^3$$

$$a = \log (100 - p) \qquad \text{for } 70\% \le p \le 99.9\%$$

Predicted values of $<T_D>$ and $<T_I>$ for 99% of the time at elevation angles from 5° to 10° are 0.05 to 0.4 s for $<T_D>$ and 5 to 40 s for $<T_I>$.

The probability density function of T_D and T_I at any time percentage ranging from 50% to 99% is approximately an exponential distribution.

5 Interference from adjacent satellite systems

5.1 General

In mobile-satellite communication systems, amplitudes of the desired signal from the satellite and an interfering signal from an adjacent satellite experience independent level fluctuations due to multipath fading, requiring a different treatment from that of fixed-satellite systems. A main point to be considered is the statistics of differential fading, which is the difference between amplitudes of the direct wave and interference wave, both affected by multipath fading.

FIGURE 5

Fade duration and fade occurrence interval

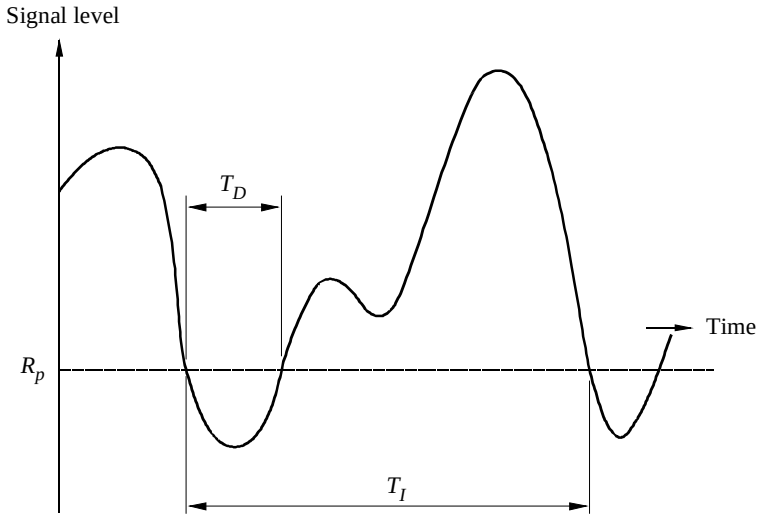

R_p: signal level for a given percentage of the time

0680-05

A practical prediction method for the statistics of signal-to-interference ratio where the effect of thermal noise and time-variant interference is taken into account is provided below.

5.2 Prediction method

In general there are two kinds of interference between adjacent satellite systems. One is “down-link interference” on the mobile earth station side, and the other is “up-link interference” on the satellite side. Another situation is interference between beams in multi-spot-beam operation, where the same frequency is allocated repeatedly. The method is applicable to such cases.

Input parameters (in units of power, not dB) are:

D: power of the direct wave component of desired signal

M: average power of the reflected component (i.e. incoherent component) of desired signal

N: average power of system noise

I_D: power of the direct wave component of interference signal

I_M: average power of reflected component of interference signal

(I: average power of interference: $I = I_D + I_M$)

Output parameters (in units of power, not dB) are:

$[c/n](p)$: ratio of desired signal power to system noise power as a function of time percentage p

$[c/i](p)$: ratio of desired signal power to interfering signal power

$[c/(i+n)](p)$: ratio of desired signal power to system noise plus interfering signal power.

Carrier-to-noise ratio as a function of p is given by:

$$[c/n](p) = (\eta_c)^2(p)\ D/N \tag{5}$$

where η_c is the normalized time-percentage-dependent factor of desired signal power having a probability density function of a Nakagami-Rice distribution with constant direct power given in Fig. 3, in which:

$$20 \log \eta_c = A + 10 \log ((D + M)/D) \tag{6}$$

where A is amplitude (dB) read from the ordinate of Fig. 3. The parameter in the figure for this application is $M/(D+M)$.

The signal-to-interference ratio as a function of p is given by:

$$[c/i](p) = (\eta_{c/i})^2(p)\ D/I_{50} \tag{7}$$

where I_{50} is the median value (i.e. value for 50% of the time) of power variations of the interference signal:

$$I_{50} = (\eta_{i,50})^2\ I \tag{8}$$

and $\eta_{c/i}$ is the normalized time-percentage-dependent factor of $[c/i]$ variations approximately given by:

$$[\log \eta_{c/i}(p)]^2 = [\log \eta_c(p)]^2 + [\log \eta_i(100 - p)]^2 \tag{9}$$

where η_i is the normalized time-percentage-dependent factor of interference signal power. A solution where $\eta_{c/i} < 1$ should be selected for the time percentage satisfying $\eta_c < 1$ and $\eta_i > 1$. By setting $I_D/I = b$, $\eta_{I,50}$ and η_i (both in dB) as a function of b are given in Table 3.

Finally,

$$[c/(i+n)](p) = [1/[c/n](p) + 1/[c/i](p)]^{-1} \tag{10}$$

Prediction accuracy of the method for $[c/i]$ and $[c/(n+i)]$ is within 1 dB for all cases within the following parameter range:

$$N \leq -5 \text{ dB}; \qquad M \leq -5 \text{ dB}; \qquad I \leq -10 \text{ dB}; \qquad 0.5 \leq b \leq 1 \tag{11}$$

where all quantities are relative to D.

TABLE 3

Values of η_i and $\eta_{I,50}$ as functions of time percentage (p) and $b = [I_D / (I_D + I_M)]$

b	I_M / I_D (dB)	$\eta_{I,50}$ (dB)	η_i (dB)							
			p(%) 50	20	10	5	1	0.5	0.1	0.01
0	∞	–1.59	0.00	3.66	5.21	6.36	8.22	8.83	9.98	11.25
0.5	0	–1.12	0.00	3.16	4.48	5.44	7.03	7.54	8.52	9.60
0.6	–1.8	–0.91	0.00	2.88	4.09	4.99	6.46	6.95	7.87	8.90
0.7	–3.7	–0.68	0.00	2.53	3.62	4.43	5.78	6.22	7.08	8.03
0.8	–6.0	–0.45	0.00	2.10	3.03	3.72	4.90	5.30	6.07	6.92
0.9	–9.5	–0.22	0.00	1.52	2.21	2.76	3.69	4.00	4.62	5.32
0.95	–12.8	–0.11	0.00	1.09	1.61	2.02	2.74	2.99	3.48	4.02
1.0	–∞	–0.00	0.00	0.00	0.00	0.00	0.00	0.00	0.00	0.00